

Entanglement of semiflexible polyelectrolytes: Crossover concentrations and entanglement density of sodium carboxymethyl cellulose

Carlos G. Lopez

Citation: *Journal of Rheology* **64**, 191 (2020); doi: 10.1122/1.5127015

View online: <https://doi.org/10.1122/1.5127015>

View Table of Contents: <https://sor.scitation.org/toc/jor/64/1>

Published by the [The Society of Rheology](#)

ARTICLES YOU MAY BE INTERESTED IN

[Operating windows for oscillatory interfacial shear rheology](#)

Journal of Rheology **64**, 141 (2020); <https://doi.org/10.1122/1.5130620>

[A slip-link model for rheology of entangled polymer melts with crystallization](#)

Journal of Rheology **64**, 213 (2020); <https://doi.org/10.1122/1.5124383>

[Design, operation, and validation of a microrheology instrument for high-pressure linear viscoelasticity measurements](#)

Journal of Rheology **64**, 205 (2020); <https://doi.org/10.1122/1.5126682>

[Horizontal extensional rheometry \(HER\) for low viscosity polymer melts](#)

Journal of Rheology **64**, 177 (2020); <https://doi.org/10.1122/1.5134532>

[Conformation and dynamics of flexible polyelectrolytes in semidilute salt-free solutions](#)

The Journal of Chemical Physics **148**, 244902 (2018); <https://doi.org/10.1063/1.5024242>

[Modeling nonlinear rheology of unentangled polymer melts based on a single integral constitutive equation](#)

Journal of Rheology **64**, 129 (2020); <https://doi.org/10.1122/1.5128295>



The advertisement features a composite image. On the left, a young child in a blue shirt is performing a split leap on a dark surface, with red laser lines extending from their feet across the floor. In the center, two Anton Paar rheometers are shown. The text 'True powder rheology' is prominently displayed in the upper right. The Anton Paar logo and name are in the bottom right corner. A 'Find out more' button is located at the bottom center.

True powder rheology

Anton Paar

Find out more



Entanglement of semiflexible polyelectrolytes: Crossover concentrations and entanglement density of sodium carboxymethyl cellulose

Carlos G. Lopez^{a)}

Institute of Physical Chemistry, RWTH Aachen University, Landoltweg 2, 52056 Aachen, Germany

(Received 7 September 2019; final revision received 1 December 2019; published 2 January 2020)

Abstract

Viscosity data for aqueous solutions of sodium carboxymethyl cellulose (NaCMC) as a function of polymer concentration (c), added salt concentration (c_S), and degree of polymerization (N) are presented. In dilute solution, NaCMC adopts an expanded coil conformation in excess salt ($R \propto N^{0.59}$, $[\eta] \sim N^{0.786}$) and a rodlike conformation ($R \propto N$, $[\eta] \sim N^2$) in salt-free water. The total persistence length in 0.1M NaCl is calculated from the N dependence of the intrinsic viscosity to be $l_p \simeq 5.5$ nm. The entanglement crossover, evaluated from the c and N dependence of the specific viscosity, is found to be independent of c_S . Our results suggest that polymer conformation (e.g., l_p or solvent quality) within the range of parameters studied does not affect the formation of entanglements. The scaling model of Dobrynin *et al.* correctly describes the nonentangled rheology of NaCMC in salt-free and excess salt solutions but does not explain the c_S independence of the entanglement crossover. Modifications to this model are proposed, which result in better but still limited agreement with experiments. © 2020 The Society of Rheology. <https://doi.org/10.1122/1.5127015>

I. INTRODUCTION

Entanglement in solutions and melts of polymers heavily slows down the dynamics of chains [1]. Beyond a certain length scale, known as the tube diameter, transverse fluctuations of polymer chains become restricted by the topological constraints imposed by other chains, and polymer diffusion occurs principally along the tube [2].

A rheological signature of entanglement is the emergence of a plateau in the storage modulus, analogous to that observed in cross-linked polymeric materials. Graessley and Edwards [3], using dimensional analysis, relate the height of entanglement plateau (G_p) to the molecular characteristics of polymers as

$$G_p l_K^3 / (k_B T) \simeq K (l_K^2 \rho L)^\alpha, \quad (1)$$

where l_K is the Kuhn length of the polymer, ρ is the number density of chains, L is their contour length, K is an unspecified constant, and $\alpha \simeq 2-2.3$ is found from experimental data [4–10].

Equation (1) was explained by the theories of Kavassalis–Lin–Noolandi [11–13] for polymer melts based on “packing” arguments. These models posit that an entanglement is formed when a fixed number of chains occupy a given volume. While this number could not be predicted from molecular architecture, analysis of neutron scattering and rheological data for flexible polymers initially suggested that it was a universal constant. Colby and Rubinstein [14] developed a different conjecture, where a fixed number of binary contacts between chains were assumed to lead to the

formation of an entanglement. The Colby–Rubinstein theory, also known as “two-parameter scaling,” successfully explained the concentration dependence of the plateau modulus of polymer solutions in good and θ solvents, predicting $G_p \propto c^{2.3}$ for both cases.

Milner [15,16] proposed some modifications to the Colby–Rubinstein approach to calculate the number of binary contacts between polymer chains in solution, without modifying the conjecture of entanglement formation put forward in [14]. The updated theory was able to quantitatively explain the entanglement density of nonionic polymer solutions based on melt rheology data, without the need for any additional free parameters.

The two-parameter scaling was applied to polyelectrolyte solutions by Dobrynin *et al.* [17], who predicted a number of unusual rheological features for polyelectrolytes, particularly under low salt conditions, such as the existence of a semidilute, nonentangled regime spanning several orders of magnitude in polymer concentration [18]. While the model of Dobrynin *et al.* has been shown to give a quantitative description of polyelectrolyte conformation, several of its predictions for entangled polyelectrolyte solutions are at odds with experimental data [19].

Carboxymethyl cellulose, commonly used as its sodium salt, is a weak, semiflexible, strongly charged polysaccharide employed as a rheology modifier in food [20–24] and pharmaceutical [25] products and in drilling muds [26–28]. Light [29,30] and small-angle neutron scattering [31,32] and light scattering data show that sodium carboxymethyl cellulose (NaCMC) is molecularly dissolved in salt-free water and aqueous NaCl solutions. For highly substituted samples [degree of substitution (DS) $\gtrsim 1$], NaCMC displays hydrophilic behavior [31]. Lowering the DS below $\simeq 0.8-0.9$ leads to associative behavior [32–34] at sufficiently high

^{a)}Electronic mail: lopez@pc.rwth-aachen.de

concentrations, resulting in strong power laws of the specific viscosity ($\eta_{sp} \sim c^{5-7}$) with concentration and eventual gelation [32,35].

In this article, data for the entanglement properties of a model polyelectrolyte, NaCMC, are presented, and the experimental results are compared with the Dobrynin model. Further, Milner's ideas are applied to polyelectrolyte solutions, and it is shown that these qualitatively modify the behavior predicted by the model of Dobrynin *et al.* Applying these modifications leads to better but still limited agreement with experiments. All the samples considered in this study are in a DS and concentration region where hydrophobic effects do not show any significant effect on the solution rheology.

II. POLYELECTROLYTE CONFORMATION AND DYNAMICS

In this section, scaling models for polyelectrolyte solutions are reviewed, commenting on the degree of experimental validation for different predictions. The conformational properties follow the de Gennes–Pfeuty–Dobrynin model [17,36,37]. Entanglement properties are calculated according to the Colby–Rubinstein theory [1,14], following the work of Dobrynin *et al.* [17]. In the discussion, the modifications introduced by Milner [15] to the Colby–Rubinstein theory of entanglement as well as the effects of intrinsic stiffness on polyelectrolyte conformation are considered.

A. Statics

1. Salt-free

According to the model of Dobrynin *et al.* [17], polyelectrolytes in dilute salt-free solution adopt an extended, rodlike conformation with an end-to-end distance of [17]

$$R = b'N, \quad (2)$$

where b' is the effective monomer size and N is the degree of polymerization. The overlap concentration marks the cross-over to the semidilute regime and is calculated by assuming that the polymer coils are space filling,

$$c^* \simeq \frac{N}{R^3} \sim \frac{1}{b'^3 N^2}, \quad (3)$$

where c^* is in units of monomers per unit volume. For $c > c^*$, polymers assume dilutelike statistics on lengthscales shorter than the mesh size or correlation length (ξ) and meltlike (Gaussian) statistics on larger ones. The correlation length varies as

$$\xi = (b'c)^{-1/2}, \quad (4)$$

with each chain containing $g_\xi(c/c^*)^{1/2}$ correlation blobs. The end-to-end distance of a chain scales as

$$R(c) \simeq N^{1/2}(c/b')^{-1/4}. \quad (5)$$

These scaling laws are in reasonably good agreement with experimental [18,31,32,38–45] and simulation [46,47] data for flexible and semiflexible polyelectrolytes. In particular,

Eqs. (4) and (5) quantitatively describe the correlation length and chain size of sodium polystyrene sulfonate (NaPSS) in salt-free water [18,39,48–50]. The conformation of salt-free polyelectrolytes has only been thoroughly investigated for NaPSS, and it is not known whether these scaling laws also apply to other systems.

2. Excess salt

In excess added salt ($fc \ll 2c_S$, where f is the fraction of dissociated counterions), electrostatic repulsion becomes short ranged [51], and its effect is similar to that of excluded volume [17,37,52,53]. Polyelectrolytes are then analogous to neutral polymers in good solvent [17,19,45,46], but their excluded volume strength can be up to several orders of magnitude larger than that of neutral polymers in the athermal solvent [1,54]. The de Gennes–Pfeuty–Dobrynin scaling theory models the persistence length of polyelectrolytes as purely electrostatic and equal to [17]

$$l_{p,D} = \frac{(cb')^{-1/2}}{2} \left(1 + \frac{2c_S}{fc}\right)^{-1/2}, \quad (6)$$

where the subscript D is used to denote that this persistence length refers to the prediction of Dobrynin *et al.* Equation (6) is in good agreement with experimental data for NaPSS in salt-free solution [18]. In excess added salt, Spiteri *et al.* [42] find $l_p \propto c_S^{-1/3}$, which is a weaker dependence than expected by Eq. (6) and is possibly related to the influence of intrinsic stiffness as discussed in [42]. The overlap concentration ($c^* \simeq N/R^3$) in the high N limit is then predicted by Dobrynin *et al.* to scale as

$$c^* \simeq (2b'^2 c_S / f)^{0.6} N^{-0.764}.$$

The $c^* \propto N^{-0.764} c_S^{0.6}$ dependence has been experimentally observed for flexible polyelectrolytes [40,55,56]. Semiflexible polyelectrolytes show a weaker c_S dependence ($c^* \sim c_S^{0.1-0.4}$) due to the non-negligible contribution of the intrinsic persistence length, but a similar N dependence [52,53]. The conformational and transport properties of dilute polyelectrolytes in solution can be described by assuming that the total persistence length is the sum of an intrinsic (or bare) contribution, $l_{p,0}$, and an electrostatic one, $l_{p,e}$ [52,56–60]. While there is no precise definition of what constitutes a flexible vs a semiflexible polyelectrolyte, for practical purposes, most polyelectrolytes with $l_{p,0} \lesssim 1$ nm can be considered flexible, because in aqueous solution the polymer rigidity arises primarily from electrostatic interactions. Polyelectrolytes with $l_{p,0} \gtrsim 5$ nm can be considered semiflexible because intrinsic rigidity tends to dominate except a very low ionic strengths (e.g., in salt-free solution).

The correlation length in the presence of added salt scales as

$$\xi \simeq (b'c)^{-1/2} [1 + 2c_S/(fc)]^{1/4}, \quad (7)$$

which has not been verified experimentally. The scaling of

Dobrynin *et al.* expects that chains are random walks of correlation blobs with an end-to-end distance of

$$R(c) \simeq N^{1/2}(c/b')^{-1/4}[1 + 2Ac_S/(fc)]^{-1/8}. \quad (8)$$

B. Unentangled dynamics

In dilute excess salt solution, the viscosity of polyelectrolyte solutions is described by the Huggins equation,

$$\eta_{sp} = c[\eta] + k_H(c[\eta])^2, \quad (9)$$

where $[\eta]$ ($= 1/c^*$) is the intrinsic viscosity and k_H is the Huggins coefficient. For salt-free polyelectrolyte solutions, Eq. (9) does not apply and c^* can be estimated instead from $\eta_{sp}(c^*) = 1$ [2,40,53].

Above c^* but below the entanglement concentration, the dynamics of polyelectrolyte solutions are Zimm-like for distances smaller than ξ and Rouse-like for larger ones. The specific viscosity is predicted to vary as [17]

$$\eta_{sp}(c) \simeq \eta_{sp}(c^*)(c/c^*)^{1/(3\nu-1)} \sim Nc^{1/(3\nu-1)}, \quad (10)$$

which, using $\eta_{sp}(c^*) = 1$ and $\nu = 1$ for salt-free solutions, leads to $\eta_{sp} \simeq Nb^{3/2}c^{1/2}$. The square-root dependence of the specific viscosity with concentration, known as the Fuoss law, has been observed for a range of nonentangled polyelectrolyte-solvent systems [18,41,55]. Deviations to both higher [19,31,53,61–63] and lower [40] exponents have also been reported. The N exponent of η_{sp} in salt-free solution has been found to be $\simeq 20$ – 40% higher than predicted by Eq. (10) [18,53]. For solutions in excess salt, the viscosity at the overlap is $\eta_{sp}(c^*) = 1 + k_H$ and $\nu = 0.59$ [64]. Equation (10) yields $\eta_{sp} \simeq (1 + k_H)(c[\eta])^{1.25}$, in agreement with experiments on flexible and semiflexible polyelectrolytes [53,55].

C. Entanglement crossover and density

The Colby–Rubinstein theory [1,65] conjectures that an entanglement is formed by a fixed number of binary contacts per entanglement strand (C^3). The density of binary contacts in solution is estimated as $\rho_b \sim \xi^{-3}$, and the average distance between them is $d_b \sim \rho_b^{-1/3} \sim \xi$. The swept volume of an entanglement strand is a^3 , and, therefore,

$$a^3 \rho_b \sim a^3 \xi^{-3} = C^3. \quad (11)$$

The last relation implies the proportionality of the tube diameter a and the correlation length [66]. Polymer chains become entangled when the chain size equals the size of the entanglement tube diameter,

$$a(c_e) = C\xi(c_e) \simeq R(c_e). \quad (12)$$

The entanglement concentration can be calculated from the variation of R and ξ with polymer concentration and Eq. (12) as

$$c_e = C^{6\nu-2}c^*. \quad (13)$$

The proportionality between the overlap and entanglement concentrations is observed for neutral polymers in good solvent and polyelectrolytes in excess salt [2,53,67] ($\nu \simeq 0.59$) but not for polyelectrolytes in salt-free solution ($\nu = 1$) [19,40,53,55].

The volume occupied by an entanglement strand is $\simeq \xi a^2$ and their number density $\rho_a \simeq (\xi a^2)^{-1}$. Assuming a plateau modulus of $k_B T$ per entanglement strand yields

$$G_{P,D} \simeq \frac{k_B T}{C^2 \xi^3}, \quad (14)$$

which is proportional to Eq. (1) with $\alpha = 3\nu/(3\nu - 1)$ and subscript D denotes that this is the prediction of the model of Dobrynin *et al.* [17]. The plateau modulus is then expected to vary as $G_p \propto c^{2.3}$ for neutral polymers in good solvent and polyelectrolytes in excess salt, in agreement with experimental results [2], and $G_p \propto c^{1.5}$ for polyelectrolytes in salt-free solution, which has not clearly been established experimentally [38,40]. Note that, since for flexible polyelectrolytes in salt-free solution, the correlation length and the persistence length are equivalent (this is predicted by the scaling of Dobrynin *et al.* [17] and has been verified experimentally for NaPSS [18]), substituting $\xi \simeq l_{p,D} \propto c^{-1/2}$ [Eq. (4)] into Eq. (1) leads to $G_p \propto c^{3/2}$ independent of the value of α . As salt is added, l_p decreases and ξ increases so that the $l_p \simeq \xi$ approximation used in salt-free solution is no longer valid. Substituting Eq. (7) into Eq. (14) gives $G_{P,D} \propto c_S^{-3/4}$, in contrast with the experimentally observed $G \propto c_S^0$ [19,45,62,68].

Data by Raspaud *et al.* [69] for polystyrene, polybutadiene, and polyisoprene in different solvents agree with Eq. (14) if a different value of C is used for each polymer-solvent pair. In order to account for this variation in C , Milner [15] proposed a correction to the scaling assumption of $\rho_b \sim \xi^{-3}$, which is discussed in Sec. V B.

D. Entangled dynamics

Above c_e , the specific viscosity is predicted by the reptation model to vary as [1,17]

$$\eta_{sp} \simeq \eta_R(c) \left(\frac{c}{c_e} \right)^{2/(3\nu-1)} \propto N^3 c^{3/(3\nu-1)}, \quad (15)$$

where $\eta_R(c)$ corresponds to the unentangled viscosity, given by Eq. (10). Note that for theta solvents, the above arguments do not apply and an alternative scaling must be used [65]. In the above discussion, tube length fluctuations have been neglected; these are known to lead to slightly higher exponents for η with N [1]. The degree of agreement of Eq. (15) with experimental results is discussed further in Sec. IV.

The specific viscosity of neutral polymers and polyelectrolytes in excess salt is empirically well described across a broad concentration range by an expanded Huggins equation, as proposed by Kulicke and co-workers [70,71],

$$\eta_{sp} = c[\eta] + k_H(c[\eta])^2 + B(c[\eta])^m, \quad (16)$$

where B is left as a free parameter and m is the exponent of the viscosity with concentration in the entangled region.

III. MATERIALS AND METHODS

A. Samples

Sodium carboxymethylcellulose samples were purchased from Sigma-Aldrich. Their nominal and measured characteristics are summarized in Table I. One sample was ultrasonically degraded to reduce its molar mass as described below. Samples were purified by precipitation or dialysis against de-ionized (DI) water to remove any residual salt present in the powder. Solutions were prepared gravimetrically by mixing the appropriate amount of polymer and solvent, followed by the use of a vortex or roller mixer to promote dissolution. The samples considered in our study do not exhibit thixotropy or phase separation upon heating/cooling. Contrary to early literature reports [72,73], it was found that the viscosity of NaCMC in salt solutions is independent of the order of polymer/salt addition. Following the earlier work, we assume a water content of 14% in the NaCMC powders [31].

B. Rheology

Rheological measurements were performed on a stress controlled Kinexus-Pro rheometer (Malvern). Two cone and plate geometries with an angle of 1° and diameters of 40 or 60 mm were employed. The temperature was controlled with a Peltier plate. A solvent trap was used to minimize sample evaporation. Measurements were carried out in steady shear for a fixed range of shear-rate values. The range of shear rates studied was varied depending on the sample concentration and molar mass to include values in the Newtonian plateau. No extrapolation was, therefore, required to obtain the zero-shear-rate viscosity. All measurements were carried out at $T = 298$ K. We have restricted measurements to $\eta_{sp} \gtrsim 1$, where the rheometer employed offers reasonable accuracy.

C. Ultrasonic degradation

Ultrasonic treatment was started out at room temperature. The bath temperature was observed to rise a few degrees as the treatment proceeded. The total ultrasonication time ($\simeq 50$ h) was delivered over the course of one week, after which the sample was dialyzed against DI water and freeze dried.

TABLE I. Characteristics of different polymers studied. Samples were purchased from Sigma-Aldrich. M_0 is the molar mass of the NaCMC monomer.

Sample	M_w (g/mol)	$[\eta]$ (M^{-1})	DS	M_0 (g/mol)	Notes
CMC85k	8.5×10^4	49	0.9 ^a	234	
CMC94k	9.4×10^4	55	0.81 ^a	227	
CMC145k	1.45×10^5	70	1.35	270	Ultrasonically degraded from CMC240k
CMC240k	2.4×10^5	110	1.35 ^b	270	Data from [19,75] and this work

^aManufacturer's specification, which is usually close to the value determined by other methods [32,74].

^bMeasured by back titration. DS is assumed to be unchanged by ultrasonic treatment.

D. Determination of degree of polymerization

The degree of polymerization N was determined from their intrinsic in 0.1M NaCl solution. Zero-shear-rate viscosity data at $T = 298$ K were measured using a cone and plate setup as described above, and the intrinsic viscosities were calculated using the Huggins equation with $k_H = 0.45$. The degree of polymerization was obtained from [53]

$$[\eta] = 0.29N^{0.87} 0.1M NaCl, \quad (17)$$

where $[\eta]$ is in units of inverse moles of repeating units per liter (M^{-1}). Molar masses were calculated by multiplying N by M_0 and are reported in Table I. Equation (17) was constructed from weight-averaged molar mass data of samples with a polydispersity of $\simeq 3-4$ [53,76]. Since the samples considered in this study are expected to have a similar polydispersity [53], Eq. (17) should yield approximately weight-averaged degrees of polymerization.

IV. RESULTS AND DATA ANALYSIS

Figure 1(a) shows the specific viscosity of sample CMC240k in salt-free and in 0.1M NaCl aqueous solution. The observed behavior is similar to that reported in an earlier study [53]. Figure 1(b) shows the specific viscosity of sample CMC240k as a function of polymer concentration in salt-free solution before and after ultrasonic treatment. The decrease in viscosity after ultrasonic treatment occurs due to a decrease in the molar mass of the polymer due to ultrasonic breakage of the chains. The decrease found is consistent with

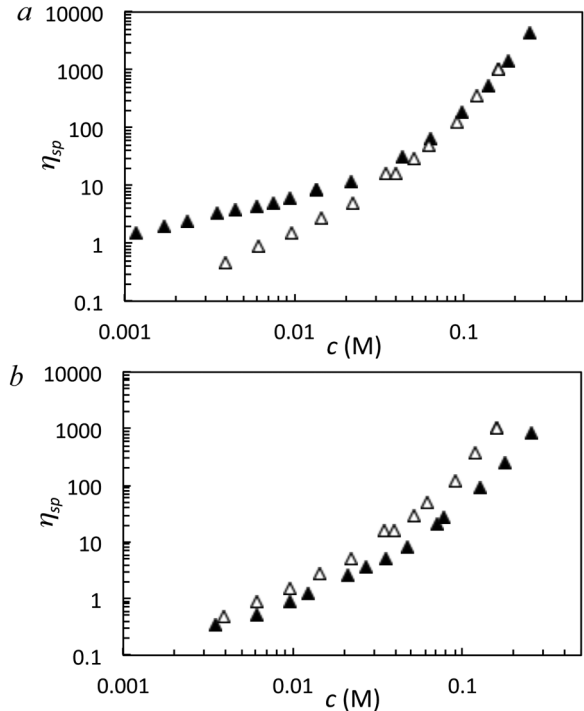


FIG. 1. Specific viscosity as a function of polymer concentration in moles of repeating units per liter. (a) CMC240k in salt-free (\blacktriangle) and 0.1M NaCl (\triangle) solutions. (b) Sample CMC240k before (\triangle) and after (\blacktriangle) ultrasonic treatment in 0.1M NaCl solution. Salt-free data for CMC240k are from [75].

the results for other cellulose derivatives [77–80] and is expected to be accompanied by a decrease in polydispersity.

Figure 2 compares the determination of c^* for three samples in DI water. The viscosity varies approximately as $\eta_{sp} \propto c^{0.68}$ for all samples. This exponent is larger than predicted by the model of Dobrynin *et al.*, in line with experimental observations for other flexible [19,38,81] and semiflexible salt-free polyelectrolyte systems [62]. The deviation from theory may arise, at least in part, due to nonuniform stretching of polyelectrolyte chains, which leads to logarithmic corrections to the chain size and correlation length [47]. Estimating the effect of these corrections at present is difficult.

A. Conformation of NaCMC in dilute solution

The applicability of the wormlike chain to polyelectrolytes in salt solution has been questioned by several authors [47,51,82]. Norisuye and co-workers have provided extensive experimental evidence showing that the conformational (radius of gyration, form factor) and transport properties (diffusion coefficient, intrinsic viscosity) of polyelectrolytes in salt solution can be accurately described the wormlike chain model [52,56–60]. Even if the applicability of the wormlike chain model to polyelectrolytes is limited, it is expected to hold at least in the high salt limit, when electrostatic forces perturb the chain conformation weakly.

Figure 3 plots the intrinsic viscosity of NaCMC in 0.1M NaCl as a function of its degree of polymerization for data from [29,30,76,83–93]. The data include NaCMC samples with $0.7 < DS < 2.4$. In agreement with the study of Barba *et al.* [30], we observe no correlation between DS and $[\eta]$ for the samples included in Fig. 3. Fits to Yamakawa’s model [94] for wormlike chains are included as lines in Fig. 3. Excluded volume effects are calculated following the same method as in [52,56,59,60]. Yamakawa’s model requires four input parameters: the total Kuhn length ($l_K = 2l_p$), the excluded volume strength (B), the cross-sectional diameter (d), and the monomer length (b'). The excluded volume strength is defined as the binary cluster integral between a pair of Kuhn segments divided by the square of the Kuhn

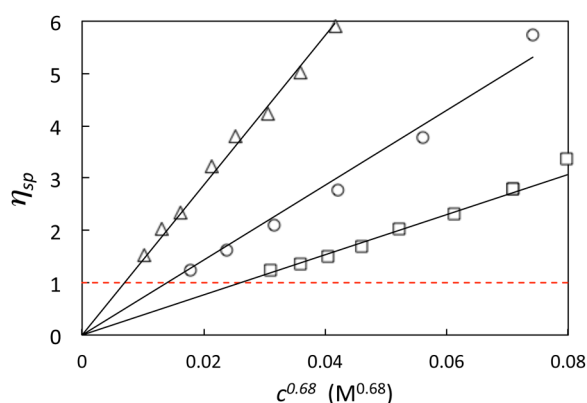


FIG. 2. Determination of overlap concentration for samples CMC240k (Δ , data from [75]), CMC145k (\circ), and CMC85k (\square) in salt-free solution. Best-fit lines are forced through the origin. c^* is estimated from the crossing of the black lines with the dashed red line, corresponding to $\eta_{sp}(c^*) = 1$.

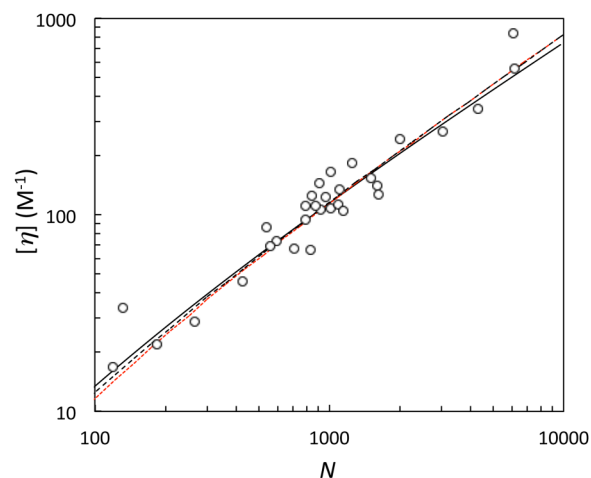


FIG. 3. Intrinsic viscosity of NaCMC in 0.1M aqueous NaCl (circles) along with fits to the wormlike chain model (lines). The parameters for the fits are as follows: full black line: $l_p = 6.5$ nm, $B = 3$ nm; dotted red line: $l_p = 5.5$ nm, $B = 4.8$ nm; dashed black line: $l_p = 4.5$ nm, $B = 6.5$ nm. $d = 1$ nm and $b' = 0.486$ nm for all three curves. Data are from [29,30,76,83–93] compiled in [53]. Data are for $T = 298$ K.

length [56]. We fix $d = 1$ nm and $b' = 0.485$ nm [31] and obtain best-fit values for l_p for different values of B . Usually, these parameters can be determined independently by observing a crossover in the power law of $[\eta]$ vs N from that of ideal chains to expanded ones. However, the data in Fig. 3 display too much scatter to determine such a change slope and, therefore, a best-fit pair of B and l_p values cannot be easily obtained. For example, setting B between 6.5 and 3 nm gives equally good fits with the corresponding values of l_p of 4.5 and 6.8 nm. In general, B for a given ionic strength does not vary strongly for highly charged polyelectrolyte systems in water. Sodium hyaluronate (NaHy) is the closest analog to NaCMC among the systems for which B has been reliably determined as a function of added salt. B is, therefore, fixed to 4.8 nm, which is the value obtained by Norisuye and co-workers [52] for NaHy at $c_s = 0.1$ M. This gives a total persistence length of $l_p \simeq 5.5$ nm, which is incompatible with the estimate of Hoogendam *et al.* [95] for the bare persistence length of $l_{p,0} \simeq 15$ nm, obtained by size exclusion chromatography coupled with light scattering. The results of Hoogendam *et al.* are in broad disagreement with viscosity [29,53,86,96–98], light scattering [29,53,86,97,98], and small-angle x-ray scattering [99] data from a large number of studies, all of which point toward a smaller bare persistence length of 5–6 nm. I do not, at this point, have an explanation for this large discrepancy.

The total persistence length is approximately $5\times$ larger than the Debye length of 0.1M NaCl ($\simeq 1$ nm), indicating that stiffness at this added salt concentration arises primarily due to the intrinsic persistence of the cellulosic backbone.

B. Concentration and molar mass exponents in semidilute solution

In an earlier study [53], three regions in the $\eta_{sp} - N - c$ parameter space of NaCMC/salt-free water were established: **I:** $\eta_{sp} \propto N^{1.4} c^{0.68}$, **II:** $\eta_{sp} \propto N^{1.8} c^{1.5}$, and **III:** $\eta_{sp} \propto N^3 c^{3.4}$.

While regime **I** could be unambiguously assigned to the semidilute nonentangled solutions, the origin of the dependences observed for **II** and **III** was less clear. The concentration dependence of $\eta_{sp} \propto c^{1.5}$ matches the prediction of Eq. (15), but the N exponent observed is too low to identify this as the entangled regime. Regime **III** has the typical N dependence of an entangled polymer solution but displays a concentration exponent significantly higher than that expected by scaling theory [17,100]. In excess salt solution, all data could be described by assuming two regimes: semidilute nonentangled and semidilute entangled (see Fig. 4).

In what follows, it is assumed that regimes **I** and **III** correspond to semidilute nonentangled and semidilute entangled solutions, respectively, and that regime **II** corresponds to a crossover between the two. There are two reasons to make these assumptions: First, scaling theory does not correctly describe several features of polyelectrolyte entanglement [19,40,53], and, therefore, one should not assign too much importance to the $\eta_{sp} \propto c^{1.5}$ prediction of Eq. (15). Second, the above assumptions allow for a consistent interpretation of all datasets considered in this work.

Figure 4 plots the specific viscosity of samples CMC240k and CMC145k in 0.1M NaCl as a function of the overlap parameter ($c[\eta]$). Equation (9) with $k_H = 0.45$ describes the data well up to $c[\eta] \simeq 3$, corresponding to $\eta_{sp} \simeq 7$. Data in $1 < c[\eta] < 3$ interval are equally well described by Eq. (10). The exponent at high concentrations tends to the previously determined value of 4, which agrees with the prediction of Eq. (15) ($\eta_{sp} \propto c^{3.9}$) for $\nu = 0.59$ [53].

C. Determination of entanglement crossover

The entanglement concentration (c_e) is estimated by fitting a crossover function,

$$\eta_{sp} = \eta_{Rouse} [1 + (c/c_e)^\beta], \quad (18)$$

where η_{Rouse} is determined by fitting the nonentangled viscosity data to a power law of $\eta_{sp} = Ac^\alpha$, where A is left as a

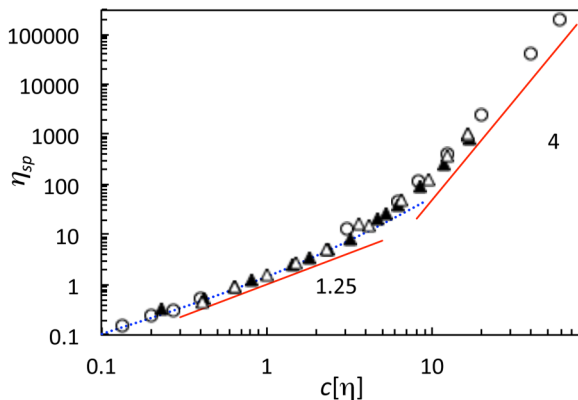


FIG. 4. Specific viscosity as a function of the overlap parameter for samples CMC240k before (\blacktriangle) and after (\triangle) ultrasonic treatment in 0.1M aqueous NaCl. Circles are the data of Barba *et al.* [30] for a 2.3×10^5 g/mol, DS = 2.4 sample. The dotted line is the Huggins equation with $k_H \simeq 0.45$. The full lines are power-law exponents for nonentangled (1.25) and entangled regimes (4).

free parameter and α is fixed at 0.68 and 1.25 for salt-free and 0.1M NaCl solutions, respectively [101]. Following the study of Lopez, the exponent β is set to 2.7 for both salt-free and 0.1M NaCl solutions, see [19,45] and references therein. The value of $\beta = 2.7$ for salt-free solutions disagrees with the prediction of $\beta = 1$ of Dobrynin *et al.* [17]. The reason for this discrepancy, as discussed in [19], is likely because the Colby–Rubinstein conjecture on entanglement formation does not hold for salt-free polyelectrolytes. The use of different crossover functions, see, for example, Eq. (10) of [102] gives very similar values of c_e .

The critical entanglement degree of polymerization (N_C) is determined from the change of the viscosity with N at a fixed polymer concentration.

$$\eta_{sp} = KN^\delta [1 + (N/N_C)^\gamma], \quad (19)$$

where the exponents δ and γ are predicted by scaling theory to be equal to 1 and 2.4, respectively, corresponding to the Rouse and reptation limit of polymer dynamics.

In excess salt solution, a value of $\delta + \gamma \simeq 3.5$ was found in an earlier study [53] in good agreement with the scaling prediction (the exponents could not be established separately). For salt-free solutions, values of $\delta \simeq 1.4 \pm 0.2$ and $\gamma \simeq 1.6 \pm 0.3$ were identified. In the present study, it is found that the N_C values obtained using the theoretical or the best-fit exponents do not differ by more than $\simeq 30\%$ and the theoretical exponents are, therefore, used.

Figure 5(a) displays the variation of the specific viscosity of NaCMC in 0.1M NaCl solution as a function of the degree of polymerization for several NaCMC concentrations, along with fits to Eq. (19) ($\delta = 1$, $\gamma = 2.4$). Data are from this study and Refs. 29–32,53,75,83,85,87,88,90,91,93 and 103–109. Figure 5(b) compares the specific viscosity as a function of the degree of polymerization for NaCMC in salt-free and 0.1M NaCl solutions at a polymer concentration of $c = 0.029$ M. In both cases, Eq. (19) describes experimental results well.

The entanglement degree of polymerization (N_e) can be estimated from the height of the G' plateau,

$$G_p = \frac{cRT}{M_0 N_e}. \quad (20)$$

This method was applied by Horinaka *et al.* [110] to NaCMC in ionic liquid 1-butyl-3-methylimidazolium acetate (BmimAc). Our investigated frequency range does not allow us to apply this method.

D. Effect of added salt on entanglement crossover

Figure 6(a) compares the overlap concentration of NaCMC in salt-free and in 0.1M NaCl solutions. The addition of salt screens electrostatic interactions and leads to a large decrease in R , with a corresponding increase in c^* . At the highest molecular weights considered ($N \simeq 5000$), the addition of 0.1M NaCl leads to an increase in c^* of over 2 orders of magnitude with respect to salt-free solution. Note that, since a best-fit exponent of $\eta_{sp} \propto c^{0.68}$ is used, these results differ slightly from those presented in [53].

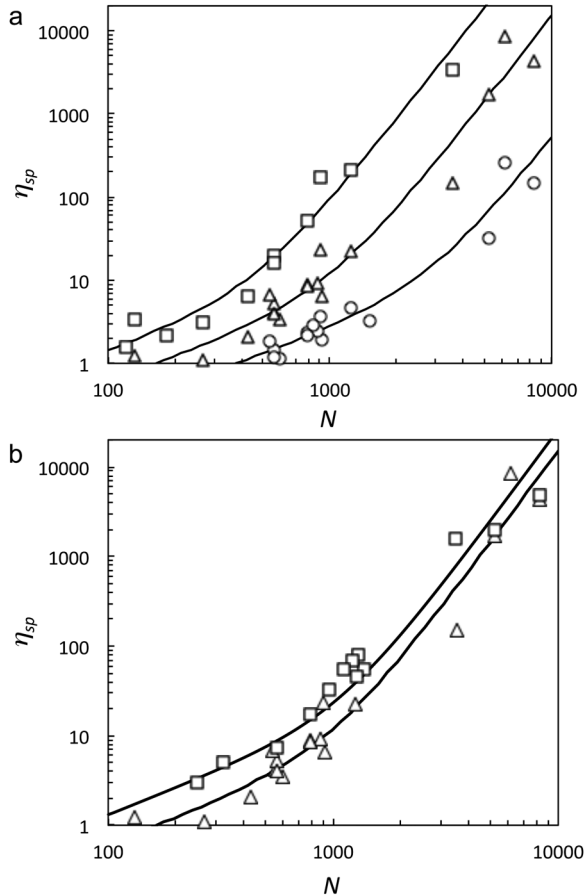


FIG. 5. Determination of the entanglement degree of polymerization for NaCMC. (a) Samples in 0.1M NaCl aqueous solution for polymer concentrations of $c = 0.064\text{M}$ (\square), $c = 0.029\text{M}$ (\triangle), and $c = 0.0124\text{M}$ (\circ). Lines are fits to Eq. (19). (b) Comparison of solutions with a polymer concentration of $c = 0.029\text{M}$ in 0.1M NaCl (\triangle) and salt-free (\square) solutions. Lines are fits to Eq. (19). Data are from this work and [29–32,53,75,83,85,87,88,90,91,93, 103–109].

Figure 6(b) shows an analogous plot for the entanglement concentration. The values extracted from Eqs. (18) and (19) agree well. In contrast to c^* , c_e is not affected by the addition of salt within the scatter of the data. This result is consistent with an earlier study [19], which showed that the entanglement concentration of an NaCMC sample with $N \simeq 1250$ was independent of added salt in the range $5 \times 10^{-6} < c_S/\text{M} < 2$.

Equating the high concentration limits of Eqs. (16) and (18) gives $c_e = [B/(1+k_H)]^{1/(\alpha-m)}[\eta]^{-1}$. Using the values of k_H , B , and m as well as the relation between $[\eta]$ and N determined in an earlier study for 0.1M NaCl [53], $c_e \simeq 5[\eta]^{-1}$ is found, which agrees well with the values plotted in Fig. 6.

The constant value of $c_e/c^* \simeq 4.5$ in 0.1M NaCl corresponds to a chain size at the entanglement concentration of $R(c_e) \simeq 0.8R(c^*) \sim N^{0.6}$, using Eq. (8). On the other hand, in salt-free solution, Eq. (5) gives $R(c_e) \sim N^{0.7}$. Thus, the end-to-end chain size at the entanglement concentration in both solvents shows a similar N dependence.

Figure 7 shows the viscosity of NaCMC solutions at the entanglement concentration as a function of degree of polymerization. In excess of added salt (0.1M NaCl), $\eta_{sp}(c_e) \simeq 25$ independent of N is observed. This constant value is

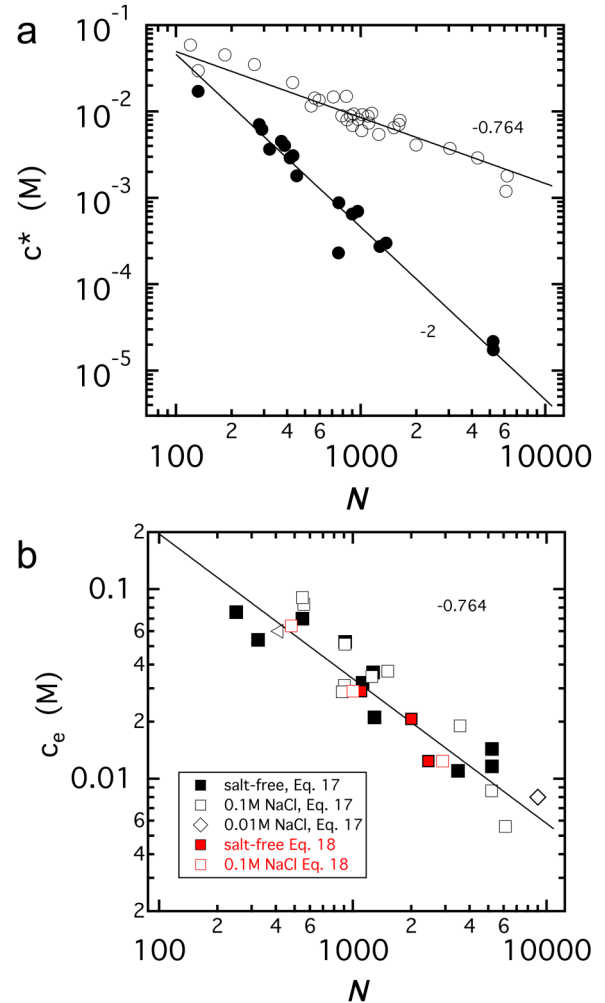


FIG. 6. Effect of added salt on overlap and entanglement parameters. (a) Overlap concentration in salt-free (full circles) and in 0.1M NaCl (hollow circles) solutions as a function of the degree of polymerization N . Data are from this work and [29–32,53,75,83–87,104,107–109,111–113] compiled in [53] and this work. Lines indicate scaling theory power laws. (b) Entanglement concentration in salt-free solution (full squares) and 0.1M NaCl solution (hollow squares). Triangle is for 2M NaCl. Line is the scaling theory prediction for polymers in good solvent. Data are from this work and [29–32,53,75,83,85,87,88,90,91,103–109] compiled in [53] and this work. Black symbols are (c_e, N) points evaluated from Eq. (18), and red symbols are (c, N_e) points evaluated from Eq. (19). See online version for color.

consistent with results for neutral polymers in good solvent [1,2,69]. In salt-free solution, the viscosity at c_e increases with the degree of polymerization.

V. DISCUSSION

Figure 8 summarizes the different concentration regimes for NaCMC following the Graessley representation [114]. The dashed lines indicate $c^* = [\eta]^{-1}$ and $c_e \simeq 4.5[\eta]^{-1}$, where $[\eta]$ is calculated using Yamakawa’s model, see Fig. 3. The entanglement crossover for salt-free and 0.1M NaCl solutions falls onto the same curve within experimental error. The onset of the concentrated regime [$\xi(c_D) = \xi_T$] is estimated to be $c_D \simeq 0.05\text{M}$ for NaCMC in 0.1M [115]. The concentrated crossover in salt-free solutions is expected to occur at a higher concentration than in 0.1M NaCl.

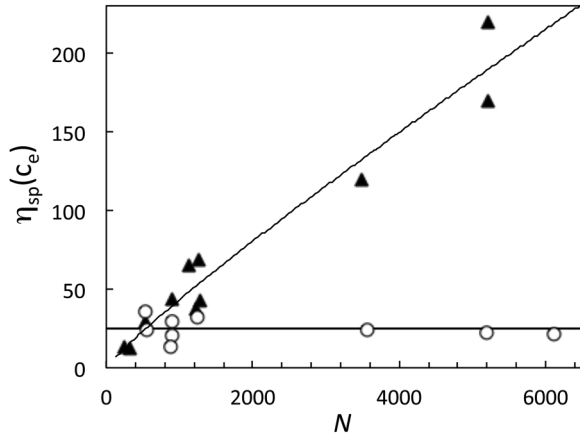


FIG. 7. Dependence of the specific viscosity at the entanglement concentration on the degree of polymerization of NaCMC. Full symbols correspond to salt-free solution and hollow symbols to 0.1M NaCl. Lines are guides to the eye. Data are from this work and references as listed in Fig. 6.

Values of the entanglement degree of polymerization (N_e) for NaCMC in BmimAc [110], calculated from Eq. (20), lie $\simeq 50\%$ above the trend observed for the critical degree of polymerization in 0.1M NaCl solution. This is consistent with data for other flexible polymers in solution, where the value of the critical molar mass [obtained from Eqs. (18) and (19)] is found to be higher than the entanglement molar mass.

Overall, rheology data point to the insensitivity of c_e , N_C , and N_e of NaCMC on the solution's ionic strength. The variation of rheological properties with added salt in semidilute entangled solution appears, therefore, to be largely the result of a change in terms outside the square brackets in Eq. (18) or the KN^γ term in Eq. (19), with the entanglement crossover and density being invariant upon changes in c_S . This interpretation is consistent with studies on other polyelectrolyte systems, which have shown that N_e does not depend on charge fraction [38,45] or c_S [19,45,62].

The observations summarized above are incompatible with the model of Dobrynin *et al.*, which predicts $c_e \propto N^{-2}$ in salt-free solution and $G_P \propto c_S^{-3/4}$ for $c > c_e$. Given these large disagreements between the experimental results and the Dobrynin model, some possible origins for the observed discrepancies are considered next. The discussion here is limited to polyelectrolyte solutions in excess of added salt, for which the dilution solution conformation is relatively well understood.

A. Static properties of semiflexible polyelectrolytes

The total persistence length of a polyelectrolyte contains an intrinsic contribution ($l_{p,0}$) and an electrostatic one ($l_{p,e}$). The intrinsic persistence length can be evaluated experimentally by extrapolation to infinite ionic strength conditions. The total persistence length is typically expressed as a sum of these two terms: $l_p = l_{p,0} + l_{p,e}$. The conformation of dilute polyelectrolytes in the added salt range of $0.005 < c_S/M < 1$ can be modeled by assuming that the electrostatic contribution varies as a power law of the Debye screening length κ^{-1} so that

$$l_p \simeq l_{p,0} + E(\kappa^{-1})^\mu. \quad (21)$$

Experimental data usually show an exponent of $\mu \simeq 0.7$ –1.3 in dilute and semidilute solutions. Note that while polyelectrolytes may adopt nonwormlike conformations, and treating l_p as a sum of two terms may not be entirely valid [82], most dilute solution experimental data can be modeled to a reasonably good accuracy using this kind of approximation [52,56–60].

Dilute solution data show that the excluded volume strength (B) depends on the Debye screening length as [52,57,60]

$$B \simeq B_0 + A\kappa^{-1}, \quad (22)$$

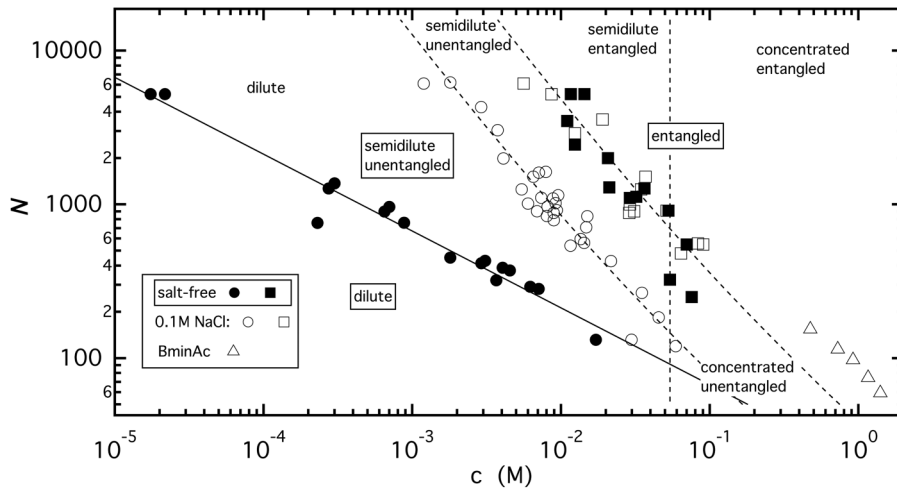


FIG. 8. Concentration regimes of NaCMC solutions in salt-free (full symbols) and 0.1M NaCl (hollow symbols) solutions, following the Graessley representation [114]. The concentrated crossover occurs when blobs have less than 130 chemical monomers. Circles and squares correspond to the overlap and entanglement crossovers, respectively. The entanglement crossover includes datapoints obtained with Eqs. (18) (c , N_C) and (19) (c_e , N). The concentration regimes for 0.1M are shown by the dashed lines and the labels without boxes. Triangles are (c , N_e) data by Horinaka *et al.* for NaCMC in BmimAc [110]. Full symbols are for salt-free solutions, and labels are in boxes.

where $A \simeq 3-6$ for highly charged aqueous systems in the $0.005 < c_S/M < 1$ range and B_0 corresponds to the hard-core repulsion between polymer segments at infinite ionic strength. Assuming a hard-core potential with a chain cross-sectional diameter d , the intrinsic contribution to the excluded volume can be approximated as $B_0 = \pi d/2$ [116]. The Dobrynin model corresponds to Eqs. (21) and (22) for $B_0 = 0$, $l_{p,0} = 0$ (intrinsically flexible polyelectrolytes), and $\mu = 1$.

Chains follow Gaussian statistics up to the thermal blob, with size

$$\xi_T = 2^{3/2} l_p g_{T,p}^{1/2}, \quad (23)$$

where $g_{T,p} = l_p/b'$ is the number of persistence lengths inside the thermal blob,

$$g_{T,p} = 8(l_p/B)^2.$$

The number of chemical monomers inside a thermal blob is, therefore, $g_T = (l_p/b')g_{T,p}$. For $N > g_T$, chains in dilute solution are an expanded coil of thermal blobs with an end-to-end distance of [1,117]

$$R \simeq \xi_T (N/g_T)^{0.59}. \quad (24)$$

The correlation length and chain size for $N > g_T$ and $\xi > \xi_T$ can be calculated using

$$\xi(c) = R(c^*)(c/c^*)^{-0.77}, \quad (25)$$

$$R(c) = R(c^*)(c/c^*)^{-0.125}. \quad (26)$$

In the following discussion, prefactors are largely dropped, focusing instead on the c_S exponents predicted by Eqs. (21)–(26). The excess salt regime is subdivided into three different regions:

Region I: For salt concentrations at which the electrostatic terms of Eqs. (21) and (22) dominate, $B \sim \kappa^{-1}$ and $l_p \sim (\kappa^{-1})^\mu$.

Region II: For semiflexible polyelectrolytes, at intermediate salt concentrations, there exists a regime for which $l_p \simeq l_{p,0}$ and $B \sim \kappa^{-1}$. For example, at $c_S = 0.1\text{M}$, $l_p \simeq 1.1l_{p,0}$, and $B \simeq 1.2B_{el}$ for NaCMC.

Region III: At very high salt concentrations, the nonionic terms of Eqs. (21) and (22) dominate and polyelectrolyte chain dimensions are nearly independent of added salt.

If (somewhat arbitrarily) the c_S value at which the cross-over between regions I and II occurs (c'_S) is set to $l_p = 1.3l_{p,0}$, c'_S can be estimated as follows:

$$c'_S = 9 \left(\frac{3E}{l_{p,0}} \right)^{2/\mu},$$

where the relation $\kappa^{-1} \simeq 0.3c_S^{-1/2}$ nm for monovalent salt aqueous solutions has been used. For NaCMC, $c'_S \simeq 0.01 - 0.03\text{M}$ is obtained.

The c_S value at which region III sets in (c''_S) can be approximated from $B \simeq 1.3B_0$, yielding

TABLE II. Dependence of some dilute solution properties with the inverse Debye screening length κ^{-1} . Number represents exponent ζ so that for a given quantity X [e.g., $X = \xi_T$, $R(c)$, etc.], $X \propto (\kappa^{-1})^\zeta$.

	I ^a	II	III
	$B \sim \kappa^{-1}$, $l_p \sim \kappa^{-\mu}$	$B \sim \kappa^{-1}$, $l_p \sim l_{p,0}$	$B \sim B_0$, $l_p \sim l_{p,0}$
R_{dilute}	$0.18 + 0.23\mu$	0.18	0
D	$-0.18 - 0.23\mu$	-0.18	0
c^*	$-0.54 - 0.69\mu$	-0.54	0
ξ	$-0.24 - 0.3\mu$	-0.24	0

^aReduces to the model of Dobrynin *et al.* [17] for $\mu = 1$. The exponent λ of the various quantities on c_S ($X \propto c_S^\lambda$) is given by $\lambda = -\zeta/2$.

$$c''_S = \left(\frac{A}{B_0} \right)^2,$$

which corresponds to $c''_S \simeq 1\text{M}$ for NaCMC.

Table II summarizes the dependence of some dilute solution properties on κ^{-1} , based on Eqs. (21), (22), and (24) for the three cases considered. Case I for $\mu = 1$ gives the exponents of the model of Dobrynin *et al.*, and for $\mu = 0$, it reduces to regime II [118]. The exponents of $R_{dilute} \propto c_S^{-0.09}$, $D \propto c_S^{0.09}$, and $c^* \propto c_S^{0.27}$ expected for regime II agree moderately well with dilute solution data for NaCMC (see Tables IV–VI in the Appendix). Overall, the data are in better agreement with the equations derived in this section for case II than they are with the equations outlined in the Introduction.

B. Revised scaling laws for polyelectrolyte entanglement

Parameter C in Eq. (11) is expected by the Colby–Rubinstein model by a constant for a given polymer-solvent pair. In order to account for this variation, Milner [15] proposed replacing C by

$$C \rightarrow C \left(\frac{l_{pck}}{\xi_T} \right)^{1/3}, \quad (27)$$

where $l_{pck} = Nb^3/[R^2(c)]$. The modified parameter C was then found to be independent of the polymer-solvent pair for the systems studied by Raspaud *et al.* [69]. Applying this correction, the plateau modulus is modified by a factor of $F = (\xi_T/l_{pck})^{2/3}$ so that

$$G_{p,M} = \left(\frac{\xi_T}{l_{pck}} \right)^{2/3} \frac{k_B T}{C^2 \xi^3}. \quad (28)$$

In the salt-free case, Milner's corrections should not apply because chains are expected to adopt Gaussian statistics at all lengthscales larger than the total persistence length. This occurs because the scaling theory expects the excluded volume interactions to be screened at the same lengthscale as the electrostatic persistence length [119].

Table III summarizes the κ^{-1} dependence of different quantities for the three excess salt scenarios considered in Sec. V A. Quantities with the subscript M refer to those where the Milner correction has been applied. As before, case I for $\mu = 1$ reduces to the predictions of the Dobrynin model.

TABLE III. Dependence of various quantities on the inverse Debye screening length κ^{-1} . Entries represent exponent ζ so that for a given quantity X [e.g., $X = \xi_T$, $R^2(c)$, etc.], $X \propto (\kappa^{-1})^\zeta$. The different exponents are calculated for the excess salt scenario so that Eqs. (7) and (8) apply. Quantities with the subscript M refer to those where the Milner correction is applied. The exponent λ of the various quantities on c_S ($X \propto c_S^\lambda$) is given by $\lambda = -\zeta/2$.

	I ^a	II	III
	$B \sim \kappa^{-1}$, $l_p \sim \kappa^{-\mu}$	$B \sim \kappa^{-1}$, $l_p \sim l_{p,0}$	$B \sim B_0$, $l_p \sim l_{p,0}$
ξ_T	$2\mu - 1$	-1	0
$R^2(c)$	$0.23 + 0.29\mu$	0.23	0
l_{pck}/ξ_T	$0.78 - 2.3\mu$	0.78	0
a_M	$0.023 - 1.1\mu$	0.023	0
$c_{e,M}$	$-0.14 - 1.9\mu$	-0.14	0
$G_p \propto \xi^{-3}$	$0.71 + 0.9\mu$	0.71	0
$G_{p,M}$	$0.19 + 2.4\mu$	0.19	0

Interestingly, Table III reveals that once the effects of the intrinsic rigidity and Eq. (27) have been taken into account, there is a broad range of added salt concentrations ($c_S > c'_S$) for which the entanglement properties ($c_{e,M}$ and $G_{p,M}$) are expected to be essentially salt-independent, in agreement with the data presented in this paper, e.g., Fig. 6(a) and earlier work [19,45]. The independence of c_e at lower salt concentrations remains unexplained. According to Table III, as the salt concentration is decreased below c'_S , a regime where $G_{p,M}$ and $c_{e,M}$ strongly depend on c_S is expected. The dependence becomes stronger as the exponent μ increases; for the OSF case ($\mu = 1$), Table III gives a dependence of $G_{p,M} \propto c_S^{-2.5}$, and for the Dobrynin case ($\mu = 1$), a weaker dependence of $G_{p,M} \propto c_S^{-1.3}$ is expected. Note that since these equations are derived in the excess salt limit [in the low salt limit, Eqs. (25) and (26) do not hold], they cannot be applied to the data in Fig. 6(a) for $c_S \lesssim 0.02\text{M}$, which roughly corresponds to c'_S . It is, therefore, not possible at this point to provide an experimental test for the predictions of regime I.

Additionally, a detailed test of the validity of these predictions would require an accurate knowledge of the parameters B_0 , A , $l_{K,0}$, D , and μ , which would allow us to establish the boundaries between the different regimes. Unfortunately, these quantities are known only approximately, and it is, therefore, not possible to properly check whether the corrections to the scaling picture outlined here are sufficient to explain some of the discrepancies between theory and experiments observed in this study.

Regime I should be most easily observed in intrinsically flexible polyelectrolyte solutions. Experimental data [38,40,68] for the variation of the entanglement density with added salt and charge density for flexible systems do not agree with the Dobrynin model or with the scaling laws presented in this section.

In summary, the experimental data discussed in this paper and in earlier literature [19,38,45] support a broad independence of the entanglement density and entanglement cross-over of flexible [38,45] and semiflexible [19] polyelectrolytes on the added salt concentration, which is not expected from the scaling of Dobrynin *et al.* Applying Milner's corrections to the Colby–Rubinstein model of polymer entanglement can

account for the observed independence of G_p and c_e on c_S only over a limited c_S . At low added salt concentrations ($c_S < c'_S$), experimental results cannot be explained by the various models considered.

VI. CONCLUSIONS

The variation of the overlap and entanglement concentrations of NaCMC as a function of added salt and molecular weight is established. Rheological data for NaCMC in salt-free water and aqueous salt solutions suggest that electrostatics only have a small influence on the entanglement properties of NaCMC despite strongly affecting its conformation. While it is possible to rationalize the independence of the entanglement properties on c_S at high added salt concentration, it is not at present possible to explain their independence in the low c_S region.

ACKNOWLEDGMENTS

The author would like to thank Professor W. Richtering (RWTH Aachen University), R. H. Colby (Pennsylvania State University), and J. S. Behra (University of Montpellier) for many useful discussions and comments on the manuscript.

APPENDIX: DILUTE SOLUTION PROPERTIES OF NaCMC

TABLE IV. Exponent λ relating the radius of gyration (R_g) to the added salt concentration: $R_g \propto c_S^\lambda$. Values in brackets correspond to using a low salt limit of 0.01M.

Reference	N	c_S (M)	λ_R
Brown <i>et al.</i> [29,103]	600–4300	0.005–0.2	0.17 (0.16)
Trap and Herrmans [120]	760	3.75×10^{-4} –0.19	0.1 (0.07)
Schneider and Doty [86]	2000	0.005–0.5	0.08 (0.06)

TABLE V. Exponent λ relating the diffusion coefficient (D) to the added salt concentration: $D \propto c_S^\lambda$. Values in brackets correspond to using a low salt limit of 0.01M. Exponent calculated assuming that D is proportional to the sedimentation coefficient for a given molecular weight.

Reference	N	c_S (M)	λ_D
Brown <i>et al.</i> [29,103]	600–4300	0.005–0.2	0.07–0.11 (0.05–0.1)
Sitaramaiah and Goring [121]	1500–3000	0.001–0.1	0.12 (0.12)

TABLE VI. Exponent λ relating the overlap concentration ($c^* \equiv [\eta]^{-1}$) to the added salt concentration: $c^* \propto c_S^{\lambda_{[n]}}$.

Reference	N	c_S (M)	$\lambda_{[\eta]}$
Brown <i>et al.</i> [29,103]	600–4300	0.005–0.2	0.2–0.27
Fujita and Homma [122]	760	2.5×10^{-4} –0.05	0.24
Schneider and Doty [86]	2000	0.005–0.5	0.24
Moan and Wolff [90]	131	9×10^{-4} –0.1	0.21
Pals and Herrmans [123]	560–1600	3.75×10^{-4} –0.192	0.24–0.27
Chatterjee and Das [124]	200	10^{-4} –0.1	0.3
Lopez <i>et al.</i> [53] (sample 320k)	1250	10^{-3} –0.01	0.39
Lopez <i>et al.</i> [53] (sample 320k)	1250	0.02–2	0.13

REFERENCES

- [1] Rubinstein, M., and R. H. Colby, *Polymer Physics* (Oxford University, Oxford, 2003).
- [2] Colby, R. H., "Structure and linear viscoelasticity of flexible polymer solutions: Comparison of polyelectrolyte and neutral polymer solutions," *Rheol. Acta* **49**(5), 425–442 (2010).
- [3] Graessley, W., and S. Edwards, "Entanglement interactions in polymers and the chain contour concentration," *Polymer* **22**(10), 1329–1334 (1981).
- [4] Heymans, N., "A novel look at models for polymer entanglement," *Macromolecules* **33**(11), 4226–4234 (2000).
- [5] Fetters, L., D. Lohse, and R. Colby, Chain dimensions and entanglement spacings, in *Physical Properties of Polymers Handbook* (Springer, Berlin, 2007), pp. 447–454.
- [6] Horinaka, J.-I., Y. Urabayashi, and T. Takigawa, "Effects of side groups on the entanglement network of cellulosic polysaccharides," *Cellulose* **22**(4), 2305–2310 (2015).
- [7] Sukumaran, S. K., G. S. Grest, K. Kremer, and R. Everaers, "Identifying the primitive path mesh in entangled polymer liquids," *J. Polym. Sci. B Polym. Phys.* **43**(8), 917–933 (2005).
- [8] Everaers, R., "Topological versus rheological entanglement length in primitive-path analysis protocols, tube models, and slip-link models," *Phys. Rev. E* **86**(2), 022801 (2012).
- [9] Shahid, T., Q. Huang, F. Oosterlinck, C. Clasen, and E. Van Ruymbeke, "Dynamic dilution exponent in monodisperse entangled polymer solutions," *Soft Matter* **13**(1), 269–282 (2017).
- [10] Van Ruymbeke, E., Y. Masubuchi, and H. Watanabe, "Effective value of the dynamic dilution exponent in bidisperse linear polymers: From 1 to 4/3," *Macromolecules* **45**(4), 2085–2098 (2012).
- [11] Lin, Y., "Number of entanglement strands per cubed tube diameter, a fundamental aspect of topological universality in polymer viscoelasticity," *Macromolecules* **20**(12), 3080–3083 (1987).
- [12] Kavassalis, T. A., and J. Noolandi, "Entanglement scaling in polymer melts and solutions," *Macromolecules* **22**(6), 2709–2720 (1989).
- [13] Kavassalis, T. A., and J. Noolandi, "New view of entanglements in dense polymer systems," *Phys. Rev. Lett.* **59**(23), 2674 (1987).
- [14] Colby, R. H., M. Rubinstein, and J. L. Viovy, "Chain entanglement in polymer melts and solutions," *Macromolecules* **25**(2), 996–998 (1992).
- [15] Milner, S., "Predicting the tube diameter in melts and solutions," *Macromolecules* **38**(11), 4929–4939 (2005).
- [16] Qin, J., and S. T. Milner, "Tube diameter of oriented and stretched polymer melts," *Macromolecules* **46**(4), 1659–1672 (2013).
- [17] Dobrynin, A. V., R. H. Colby, and M. Rubinstein, "Scaling theory of polyelectrolyte solutions," *Macromolecules* **28**(6), 1859–1871 (1995).
- [18] Lopez, C. G., and W. Richtering, "Conformation and dynamics of flexible polyelectrolytes in semidilute salt-free solutions," *J. Chem. Phys.* **148**(24), 244902 (2018).
- [19] Lopez, C. G., "Entanglement properties of polyelectrolytes in salt-free and excess-salt solutions," *ACS Macro Lett.* **8**, 979–983 (2019).
- [20] Alghooneh, A., S. M. Razavi, and S. Kasapis, "Hydrocolloid clustering based on their rheological properties," *J. Texture Stud.* **49**(6), 619–638 (2018).
- [21] Han, M., M. P. Clausen, M. Christensen, E. Vossen, T. Van Hecke, and H. C. Bertram, "Enhancing the health potential of processed meat: The effect of chitosan or carboxymethyl cellulose enrichment on inherent microstructure, water mobility and oxidation in a meat-based food matrix," *Food Funct.* **9**(7), 4017–4027 (2018).
- [22] Youssef, A. M., and S. M. El-Sayed, "Bionanocomposites materials for food packaging applications: Concepts and future outlook," *Carbohydr. Polym.* **193**, 19–27 (2018).
- [23] Liu, Y., and K. Zhao, "Rheological and dielectric behavior of milk/sodium carboxymethylcellulose mixtures at various temperatures," *J. Mol. Liq.* **290**, 111175 (2019).
- [24] Ross, A. I., P. Tyler, M. G. Borgognone, and B. M. Eriksen, "Relationships between shear rheology and sensory attributes of hydrocolloid-thickened fluids designed to compensate for impairments in oral manipulation and swallowing," *J. Food Eng.* **263**, 123–131 (2019).
- [25] Arca, H. C., L. I. Mosquera-Giraldo, V. Bi, D. Xu, L. S. Taylor, and K. J. Edgar, "Pharmaceutical applications of cellulose ethers and cellulose ether esters," *Biomacromolecules* **19**(7), 2351–2376 (2018).
- [26] Pu, W., C. Shen, B. Wei, Y. Yang, and Y. Li, "A comprehensive review of polysaccharide biopolymers for enhanced oil recovery (EOR) from flask to field," *J. Ind. Eng. Chem.* **61**, 1–11 (2018).
- [27] Kelessidis, V., E. Poulakakis, and V. Chatzistamou, "Use of carbopol 980 and carboxymethyl cellulose polymers as rheology modifiers of sodium-bentonite water dispersions," *Appl. Clay Sci.* **54**(1), 63–69 (2011).
- [28] Srungavarapu, M., K. K. Patidar, A. K. Pathak, and A. Mandal, "Performance studies of water-based drilling fluid for drilling through hydrate bearing sediments," *Appl. Clay Sci.* **152**, 211–220 (2018).
- [29] Brown, W., D. Henley, and J. Ohman, "Sodium carboxymethyl cellulose experimental study of influence of molecular weight and ionic strength on polyelectrolyte configuration," *Arkiv Kemi* **22**(3–4), 189–206 (1964).
- [30] Barba, C., D. Montané, X. Farriol, J. Desbrières, and M. Rinaudo, "Synthesis and characterization of carboxymethylcelluloses from non-wood pulps II. Rheological behavior of CMC in aqueous solution," *Cellulose* **9**(3–4), 327–335 (2002).
- [31] Lopez, C. G., S. E. Rogers, R. H. Colby, P. Graham, and J. T. Cabral, "Structure of sodium carboxymethyl cellulose aqueous solutions: A SANS and rheology study," *J. Polym. Sci. B Polym. Phys.* **53**(7), 492–501 (2015).
- [32] Lopez, C. G., R. H. Colby, and J. T. Cabral, "Electrostatic and hydrophobic interactions in NaCMC aqueous solutions: Effect of degree of substitution," *Macromolecules* **51**(8), 3165–3175 (2018).
- [33] Róžańska, S., K. Verbeke, J. Róžański, C. Clasen, and P. Wagner, "Capillary breakup extensional rheometry of sodium carboxymethylcellulose solutions in water and propylene glycol/water mixtures," *J. Polym. Sci. B Polym. Phys.* **57**, 1537–1547 (2019).
- [34] Komorowska, P., S. Róžańska, and J. Róžański, "Effect of the degree of substitution on the rheology of sodium carboxymethylcellulose solutions in propylene glycol/water mixtures," *Cellulose* **24**(10), 4151–4162 (2017).
- [35] Savadkoohi, S., and A. Farahnaky, "Small deformation viscoelastic and thermal behaviours of pomegranate seed pips CMC gels," *J. Food Sci. Technol.* **52**(7), 4186–4195 (2015).
- [36] De Gennes, P. G., P. Pincus, R. M. Velasco, and F. Brochard, "Remarks on polyelectrolyte conformation," *J. Phys. (France)* **37**(12), 1461–1473 (1976).
- [37] Pfeuty, P., "Conformation des polyelectrolytes ordre dans les solutions de polyelectrolytes," *J. Phys. Colloq.* **39**(C2), C2-149–C2-160 (1978).
- [38] Dou, S., and R. H. Colby, "Charge density effects in salt-free polyelectrolyte solution rheology," *J. Polym. Sci. B Polym. Phys.* **44**(14), 2001–2013 (2006).
- [39] Dou, S., and R. H. Colby, "Solution rheology of a strongly charged polyelectrolyte in good solvent," *Macromolecules* **41**(17), 6505–6510 (2008).
- [40] Boris, D. C., and R. H. Colby, "Rheology of sulfonated polystyrene solutions," *Macromolecules* **31**(17), 5746–5755 (1998).

- [41] Di Cola, E., N. Plucktaveesak, T. A. Waigh, R. H. Colby, J. S. Tan, W. Pyckhout-Hintzen, and R. K. Heenan, "Structure and dynamics in aqueous solutions of amphiphilic sodium maleate-containing alternating copolymers," *Macromolecules* **37**(22), 8457–8465 (2004).
- [42] Spiteri, M., F. Boué, A. Lapp, and J. Cotton, "Persistence length for a PSSNa polyion in semidilute solution as a function of the ionic strength," *Phys. Rev. Lett.* **77**(26), 5218 (1996).
- [43] Kaji, K., H. Urakawa, T. Kanaya, and R. Kitamaru, "Phase diagram of polyelectrolyte solutions," *J. Phys.* **49**(6), 993–1000 (1988).
- [44] Salamon, K., D. Aumiler, G. Pabst, and T. Vuletia, "Probing the mesh formed by the semirigid polyelectrolytes," *Macromolecules* **46**(3), 1107–1118 (2013).
- [45] Lopez, C. G., "Scaling and entanglement properties of neutral and sulfonated polystyrene," *Macromolecules* **52**(23), 9409–9415 (2019).
- [46] Dobrynin, A. V., "Theory and simulations of charged polymers: From solution properties to polymeric nanomaterials," *Curr. Opin. Colloid Interface Sci.* **13**(6), 376–388 (2008).
- [47] Liao, Q., A. V. Dobrynin, and M. Rubinstein, "Molecular dynamics simulations of polyelectrolyte solutions: Nonuniform stretching of chains and scaling behavior," *Macromolecules* **36**(9), 3386–3398 (2003).
- [48] Prabhu, V., M. Muthukumar, G. D. Wignall, and Y. B. Melnichenko, "Polyelectrolyte chain dimensions and concentration fluctuations near phase boundaries," *J. Chem. Phys.* **119**(7), 4085–4098 (2003).
- [49] Nierlich, M., C. Williams, F. Boue, J. Cotton, M. Daoud, B. Famoux, G. Jannink, C. Picot, M. Moan, C. Wolff, M. Rinaudo, and P. de Gennes, "Small angle neutron scattering by semi-dilute solutions of polyelectrolyte," *J. Phys.* **40**(7), 701–704 (1979).
- [50] Ermi, B. D., and E. J. Amis, "Domain structures in low ionic strength polyelectrolyte solutions," *Macromolecules* **31**(21), 7378–7384 (1998).
- [51] Dobrynin, A. V., and M. Rubinstein, "Theory of polyelectrolytes in solutions and at surfaces," *Prog. Polym. Sci.* **30**(11), 1049–1118 (2005).
- [52] Tsutsumi, K., and T. Norisuye, "Excluded-volume effects in sodium hyaluronate solutions revisited," *Polym. J.* **30**(4), 345–349 (1998).
- [53] Lopez, C. G., R. H. Colby, P. Graham, and J. T. Cabral, "Viscosity and scaling of semiflexible polyelectrolyte NaCMC in aqueous salt solutions," *Macromolecules* **50**(1), 332–338 (2016).
- [54] Yamakawa, H., T. Yoshizaki, and D. Ida, "A picture of dilute solution behavior of polymers through polyelectrolyte simulation," *J. Chem. Phys.* **139**(20), 204902 (2013).
- [55] Di Cola, E., T. A. Waigh, and R. H. Colby, "Dynamic light scattering and rheology studies of aqueous solutions of amphiphilic sodium maleate containing copolymers," *J. Polym. Sci. B Polym. Phys.* **45**(7), 774–785 (2007).
- [56] Yashiro, J., R. Hagino, S. Sato, and T. Norisuye, "Chain stiffness and excluded-volume effects in poly electrolyte solutions: Characterization of sodium poly (2-acrylamido-2-methylpropanesulfonate) in aqueous sodium chloride," *Polym. J.* **38**(1), 57–63 (2006).
- [57] Hirose, E., Y. Iwamoto, and T. Norisuye, "Chain stiffness and excluded-volume effects in sodium poly (styrenesulfonate) solutions at high ionic strength," *Macromolecules* **32**(25), 8629–8634 (1999).
- [58] Iwamoto, Y., E. Hirose, and T. Norisuye, "Electrostatic contributions to chain stiffness and excluded-volume effects in sodium poly (styrenesulfonate) solutions," *Polym. J.* **32**(5), 428–434 (2000).
- [59] Hayashi, K., K. Tsutsumi, T. Norisuye, and A. Teramoto, "Electrostatic contributions to chain stiffness and excluded-volume effects in sodium hyaluronate solutions," *Polym. J.* **28**(10), 922–928 (1996).
- [60] Yashiro, J., and T. Norisuye, "Excluded-volume effects on the chain dimensions and transport coefficients of sodium poly (styrene sulfonate) in aqueous sodium chloride," *J. Polym. Sci. B Polym. Phys.* **40**(23), 2728–2735 (2002).
- [61] Rodríguez-Rivero, C., L. Hilliou, E. M. M. del Valle, and M. A. Galán, "Rheological characterization of commercial highly viscous alginate solutions in shear and extensional flows," *Rheol. Acta* **53**(7), 559–570 (2014).
- [62] Mo, Y., T. Takaya, K. Nishinari, K. Kubota, and A. Okamoto, "Effects of sodium chloride, guanidine hydrochloride, and sucrose on the viscoelastic properties of sodium hyaluronate solutions," *Biopolymers* **50**(1), 23–34 (1999).
- [63] Yu, F., F. Zhang, T. Luan, Z. Zhang, and H. Zhang, "Rheological studies of hyaluronan solutions based on the scaling law and constitutive models," *Polymer* **55**(1), 295–301 (2014).
- [64] We use $\eta_{sp}(c^*) = 1 + k_h$ in excess salt where the Huggins equation applies, following the approximation $c^* = [\eta]^{-1}$. In salt-free solution, where the Huggins equation cannot be used, we use $\eta_{sp}(c^*) = 1$, following Colby and co-workers [40,41].
- [65] Colby, R. H., and M. Rubinstein, "Two-parameter scaling for polymers in θ solvents," *Macromolecules* **23**(10), 2753–2757 (1990).
- [66] Note that for θ solvents the above reasoning does not apply because the correlation length is not determined by the number of binary contact in solution. Since θ solvents are not considered in this paper, this scenario is not discussed.
- [67] Fouissac, E., M. Milas, and M. Rinaudo, "Shear-rate, concentration, molecular weight, and temperature viscosity dependences of hyaluronate, a wormlike polyelectrolyte," *Macromolecules* **26**(25), 6945–6951 (1993).
- [68] Yamaguchi, M., M. Wakutsu, Y. Takahashi, and I. Noda, "Viscoelastic properties of polyelectrolyte solutions. 2. Steady-state compliance," *Macromolecules* **25**(1), 475–478 (1992).
- [69] Raspaud, E., D. Lairez, and M. Adam, "On the number of blobs per entanglement in semidilute and good solvent solution: Melt influence," *Macromolecules* **28**(4), 927–933 (1995).
- [70] Kulicke, W.-M., and R. Kniewske, "The shear viscosity dependence on concentration, molecular weight, and shear rate of polystyrene solutions," *Rheol. Acta* **23**(1), 75–83 (1984).
- [71] Clasen, C., and W.-M. Kulicke, "Determination of vis-coelastic and rheo-optical material functions of water-soluble cellulose derivatives," *Prog. Polym. Sci.* **26**(9), 1839–1919 (2001).
- [72] Yang, X. H., and W. L. Zhu, "Viscosity properties of sodium carboxymethylcellulose solutions," *Cellulose* **14**(5), 409–417 (2007).
- [73] Ott, E., and J. H. Elliott, "Observations on the thixotropy and structural characteristics of sodium carboxymethylcellulose," *Die Makromol. Chem.* **18**(1), 352–366 (1956).
- [74] Cai, Z., J. Wu, B. Du, and H. Zhang, "Impact of distribution of carboxymethyl substituents in the stabilizer of carboxymethyl cellulose on the stability of acidified milk drinks," *Food Hydrocoll.* **76**, 150–157 (2018).
- [75] Lopez, C. G., and W. Richtering, "Influence of divalent counterions on the solution rheology and supramolecular aggregation of carboxymethyl cellulose," *Cellulose* **26**(3), 1517–1534 (2019).
- [76] Arinaitwe, E., and M. Pawlik, "Dilute solution properties of carboxymethyl celluloses of various molecular weights and degrees of substitution," *Carbohydr. Polym.* **99**, 423–431 (2014).
- [77] Goodwin, D., D. Picout, S. Ross-Murphy, S. Holland, L. Martini, and M. Lawrence, "Ultrasonic degradation for molecular weight reduction of pharmaceutical cellulose ethers," *Carbohydr. Polym.* **83**(2), 843–851 (2011).
- [78] Mohod, A. V., and P. R. Gogate, "Ultrasonic degradation of polymers: Effect of operating parameters and intensification using additives for carboxymethyl cellulose (CMC) and polyvinyl alcohol (PVA)," *Ultrason. Sonochem.* **18**(3), 727–734 (2011).

- [79] Grönroos, A., P. Pirkonen, and O. Ruppert, "Ultrasonic depolymerization of aqueous carboxymethylcellulose," *Ultrason. Sonochem.* **11**(1), 9–12 (2004).
- [80] Antti, G., P. Pentti, and K. Hanna, "Ultrasonic degradation of aqueous carboxymethylcellulose: Effect of viscosity, molecular mass, and concentration," *Ultrason. Sonochem.* **15**(4), 644–648 (2008).
- [81] See the SI of [19] for a discussion of the viscosity data of [38].
- [82] Gubarev, A., J.-M. Y. Carrillo, and A. V. Dobrynin, "Scale-dependent electrostatic stiffening in biopolymers," *Macromolecules* **42**(15), 5851–5860 (2009).
- [83] Kulicke, W.-M., A. H. Kull, W. Kull, H. Thielking, J. Engelhardt, and J.-B. Pannek, "Characterization of aqueous carboxymethylcellulose solutions in terms of their molecular structure and its influence on rheological behaviour," *Polymer* **37**(13), 2723–2731 (1996).
- [84] Lohmander, U., and R. Strömberg, "Non-Newtonian flow of dilute sodium carboxymethyl cellulose solutions at different ionic strengths and of dilute solutions of cellulose nitrate and polystyrene in moderately viscous solvents studied by capillary viscometry: experimental results," *Die Makromol. Chem.* **72**(1), 143–158 (1964).
- [85] Castelain, C., J. Doublier, and J. Lefebvre, "A study of the viscosity of cellulose derivatives in aqueous solutions," *Carbohydr. Polym.* **7**(1), 1–16 (1987).
- [86] Schneider, N. S., and P. Doty, "Macro-ions. IV. The ionic strength dependence of the molecular properties of sodium carboxymethylcellulose," *J. Phys. Chem.* **58**(9), 762–769 (1954).
- [87] Meyer, F., Korrelation rheo-mechanischer und rheo-optischer Materialfunktionen, Ph.D. thesis, Universität Hamburg, Hamburg, 2008.
- [88] Rinaudo, M., J. Danhelka, and M. Milas, "A new approach to characterising carboxymethylcelluloses by size exclusion chromatography," *Carbohydr. Polym.* **21**(1), 1–5 (1993).
- [89] Pfefferkorn, P. M. J., Analytik von wasserlöslichen Polysacchariden und Polysaccharidderivaten mittels Greausschlusschromatographie kombiniert mit Viel-winkellaserlichtstreuung und Konzentrationsdetektion, Ph.D. thesis, Universität Hamburg, Hamburg, 2004.
- [90] Moan, M., and C. Wol, "Etude viscosimétrique de solutions de polyélectrolytes par dilution isoionique. effet de la densité de charge sur la conformation du polyion," *Die Makromol. Chem.* **175**(10), 2881–2894 (1974).
- [91] Charpentier, D., G. Mocanu, A. Carpov, S. Chappelle, L. Merle, and G. Müller, "New hydrophobically modified carboxymethylcellulose derivatives," *Carbohydr. Polym.* **33**(2), 177–186 (1997).
- [92] Picton, L., L. Merle, and G. Muller, "Solution behavior of hydrophobically associating cellulosic derivatives," *Int. J. Polym. Anal. Charact.* **2**(2), 103–113 (1996).
- [93] Matsumoto, T., and K. Mashiko, "Influence of added salt on dynamic viscoelasticity of CMC aqueous systems.pdf," *Polym. Eng. Sci.* **28**, 393–402 (1988).
- [94] Yamakawa, H., and M. Fujii, "Intrinsic viscosity of worm-like chains. Determination of the shift factor," *Macromolecules* **7**(1), 128–135 (1974).
- [95] Hoogendam, C. W., A. de Keizer, M. A. C. Stuart, B. H. Bijsterbosch, J. A. M. Smit, J. A. P. P. van Dijk, P. M. van der Horst, and J. G. Batelaan, "Persistence length of carboxymethyl cellulose as evaluated from size exclusion chromatography and potentiometric titrations," *Macromolecules* **31**(18), 6297–6309 (1998).
- [96] Kamide, K., M. Saito, and H. Suzuki, "Persistence length of cellulose and cellulose derivatives in solution," *Die Makromol. Chem., Rapid Commun.* **4**(1), 33–39 (1983).
- [97] Brown, W., and D. Henley, "Studies on cellulose derivatives. Part IV. The configuration of the polyelectrolyte sodium carboxymethyl cellulose in aqueous sodium chloride solutions," *Die Makromol. Chem.* **79**(1), 68–88 (1964).
- [98] Davis, R. M., "Analysis of dilute solutions of (carboxymethyl)cellulose with the electrostatic wormlike chain theory," *Macromolecules* **24**(5), 1149–1155 (1991).
- [99] Dogsa, I., M. Tomsic, J. Orehek, E. Benigar, A. Jamnik, and D. Stopar, "Amorphous supramolecular structure of carboxymethyl cellulose in aqueous solution at different pH values as determined by rheology, small angle x-ray and light scattering," *Carbohydr. Polym.* **111**, 492–504 (2014).
- [100] Muthukumar, M., "Dynamics of polyelectrolyte solutions," *J. Chem. Phys.* **107**(7), 2619–2635 (1997).
- [101] The term η_{Rouse} is used to refer to the best-fit power-law to the viscosity in the nonentangled regime. The term $\eta_{R(c)}$ refers to the scaling prediction for this quantity.
- [102] Kwon, M. K., J. Lee, K. S. Cho, S. J. Lee, H. C. Kim, S. W. Jeong, and S. G. Lee, "Scaling analysis on the linear viscoelasticity of cellulose 1-ethyl-3-methyl imidazolium acetate solutions," *Korea-Aust. Rheol. J.* **31**(3), 123–139 (2019).
- [103] Brown, W., D. Henley, and J. Öhman, "Studies on cellulose derivatives. Part I. The dimensions and configuration of sodium carboxymethyl cellulose in cadoxen and the influence of the degree of substitution," *Die Makromol. Chem.* **62**(1), 164–182 (1963).
- [104] Wu, Q., Y. Shangguan, M. Du, J. Zhou, Y. Song, and Q. Zheng, "Steady and dynamic rheological behaviors of sodium carboxymethyl cellulose entangled semi-dilute solution with opposite charged surfactant dodecyl-trimethylammonium bromide," *J. Colloid Interface Sci.* **339**(1), 236–242 (2009).
- [105] Trabelsi, S., E. Raspaud, and D. Langevin, "Aggregate formation in aqueous solutions of carboxymethylcellulose and cationic surfactants," *Langmuir* **23**, 10053–10062 (2007).
- [106] Truzzolillo, D., F. Bordini, C. Cametti, and S. Sennato, "Counterion condensation of differently flexible polyelectrolytes in aqueous solutions in the dilute and semidilute regime," *Phys. Rev. E* **79**, 011804 (2009).
- [107] Ye, T., M. Du, Y. Song, and Q. Zheng, "Effect of alkyl trimethylammonium bromide on rheology of entangled semi-dilute solution of sodium carboxymethylcellulose," *Acta Polym. Sin.* **7**, 827–834 (2015).
- [108] Lim, S., S. Kim, K. H. Ahn, and S. J. Lee, "The effect of binders on the rheological properties and the microstructure formation of lithium-ion battery anode slurries," *J. Power Sources* **299**, 221–230 (2015).
- [109] Behra, J. S., J. Mattsson, O. J. Cayre, E. S. Robles, H. Tang, and T. N. Hunter, "Characterization of sodium carboxymethyl cellulose aqueous solutions to support complex product formulation: A rheology and light scattering study," *ACS Appl. Polym. Mater.* **1**(3), 344–358 (2019).
- [110] Horinaka, J.-I., K. Chen, and T. Takigawa, "Entanglement properties of carboxymethyl cellulose and related polysaccharides," *Rheol. Acta* **57**(1), 51–56 (2018).
- [111] Tam, K., and C. Tiu, "Improved correlation for shear-dependent viscosity of polyelectrolyte solutions," *J. Non-Newtonian Fluid Mech.* **46**(2), 275–288 (1993).
- [112] Tam, K., and C. Tiu, "Steady and dynamic shear properties of aqueous polymer solutions," *J. Rheol.* **33**(2), 257–280 (1989).
- [113] Guillot, S., M. Delsanti, S. Desert, and D. Langevin, "Surfactant-induced collapse of polymer chains and monodisperse growth of aggregates near the precipitation boundary in carboxymethylcellulose-DTAB aqueous solutions," *Langmuir* **19**(2), 230–237 (2003).
- [114] Graessley, W. W., "Polymer chain dimensions and the dependence of viscoelastic properties on concentration, molecular weight and solvent power," *Polymer* **21**(3), 258–262 (1980).

- [115] The chain size is likely to decrease to some extent with increasing polymer concentration above c_D due to further screening of the electrostatic persistence length and excluded volume. In this sense, polyelectrolytes in excess salt are different from neutral polymers in good solvent.
- [116] Yamakawa, H., *Modern Theory of Polymer Solutions* (Harper & Row, New York, 1971).
- [117] A definition of thermal blob that accounts for electrostatic effects [through the first term in Eq. (22)] is used here, which differs from the standard definition, given, for example, in [1]. The concept of the electrostatic blob length is not considered because the article deals with highly charged semiflexible polyelectrolytes, see [31] for a discussion.
- [118] Note that some of the exponents differ slightly from those given in [17] because $\nu = 0.59$ is used instead of $\nu = 0.6$.
- [119] In the model of Dobrynin *et al.*, the correlation length is equivalent to twice the electrostatic persistence length in salt-free solution.
- [120] Trap, H. J. L., and J. J. Hermans, "Light-scattering by polymethacrylic acid and carboxymethylcellulose in various solvents," *J. Phys. Chem.* **58**(9), 757–761 (1954).
- [121] Sitaramaiah, G., and D. Goring, "Hydrodynamic studies on sodium carboxymethyl cellulose in aqueous solutions," *J. Polym. Sci.* **58**(166), 1107–1131 (1962).
- [122] Fujita, H., and T. Homma, "Viscosity behavior of sodium carboxymethyl cellulose in water at high dilutions," *J. Colloid Sci.* **9**(6), 591–601 (1954).
- [123] Pals, D., and J. Hermans, "Sodium salts of pectin and of carboxymethyl cellulose in aqueous sodium chloride. II Osmotic pressures," *Recl. Trav. Chim. Pays-Bas* **71**(5), 458–467 (1952).
- [124] Chatterjee, A., and B. Das, "Radii of gyration of sodium carboxymethylcellulose in aqueous and mixed solvent media from viscosity measurement," *Carbohydr. Polym.* **98**(2), 1297–1303 (2013).